

RESEARCH ARTICLE | AUGUST 08 2025

# Dynamics of a quartic Korteweg–de Vries equation with multiple dissipations via an Abelian integral approach

Xianbo Sun  ; Mingji Zhang  



Chaos 35, 083118 (2025)

<https://doi.org/10.1063/5.0269545>



## Articles You May Be Interested In

Quartic B-spline collocation method applied to Korteweg de Vries equation

*AIP Conf. Proc.* (July 2014)

A connection between HH3 and Korteweg–de Vries with one source

*J. Math. Phys.* (March 2010)

Large internal solitary waves on a weak shear

*Chaos* (June 2022)



Chaos

## Special Topics Open for Submissions

[Learn More](#)

# Dynamics of a quartic Korteweg–de Vries equation with multiple dissipations via an Abelian integral approach

Cite as: Chaos 35, 083118 (2025); doi: 10.1063/5.0269545

Submitted: 6 March 2025 · Accepted: 26 July 2025 ·

Published Online: 8 August 2025



View Online



Export Citation



CrossMark

Xianbo Sun<sup>1,a)</sup>  and Mingji Zhang<sup>2,b)</sup> 

## AFFILIATIONS

<sup>1</sup>School of Mathematics, Hangzhou Normal University, Hangzhou 311121, China

<sup>2</sup>Department of Mathematics, New Mexico Institute of Mining and Technology, Socorro, New Mexico 87801, USA

<sup>a)</sup>Also at: Department of Mathematics, Guangxi University of Finance and Economics, Nanning, Guangxi 530003, China.

<sup>b)</sup>Author to whom correspondence should be addressed: [mingji.zhang@nmt.edu](mailto:mingji.zhang@nmt.edu)

## ABSTRACT

We analyze both solitary and periodic wave solutions of a quartic Korteweg–de Vries (KdV) equation that incorporates multiple dissipative effects. The investigation primarily focuses on the dynamical behavior within a two-dimensional invariant manifold. To establish the existence of solitary waves, we employ the evaluation of the associated Abelian integral along a homoclinic loop, a method that offers significant insights into both their existence and stability. Furthermore, we rigorously derive periodic traveling waves by analyzing the dynamics induced by degenerate Hopf bifurcations, homoclinic bifurcations, and Poincaré bifurcations. These bifurcations play a pivotal role in identifying the conditions under which a unique periodic traveling wave arises and scenarios where two distinct periodic waves coexist. Notably, we also examine the intriguing coexistence of a solitary wave and a periodic wave. This comprehensive analysis sheds light on the intricate dynamics of the KdV equation under the influence of multiple dissipative mechanisms, enriching our understanding of its complex wave phenomena.

Published under an exclusive license by AIP Publishing. <https://doi.org/10.1063/5.0269545>

Wave dynamics in nonlinear systems play a crucial role in many physical phenomena, ranging from fluid dynamics to plasma physics. In this study, we investigate the quartic Korteweg–de Vries (KdV) equation, which models wave propagation under the influence of multiple dissipative effects. By employing an Abelian integral approach, we analyze the conditions for the existence and stability of both solitary and periodic traveling waves. Our results reveal intricate bifurcation structures, including degenerate Hopf bifurcations, homoclinic bifurcations, and Poincaré bifurcations, which dictate the emergence of distinct wave patterns. Notably, our findings demonstrate that two periodic traveling waves can coexist, contrasting with the previously established uniqueness results for KdV-like equations. Additionally, we identify scenarios where a solitary wave and a periodic wave can coexist. This research provides deeper insights into the complex interplay of dissipation and nonlinearity in wave systems, advancing our understanding of nonlinear wave phenomena in various scientific and engineering contexts.

## I. INTRODUCTION

Over the past few decades, numerous nonlinear evolution equations have been proposed to model a wide range of nonlinear phenomena across various fields, including shallow water wave motions in fluid dynamics, ion acoustic waves in plasmas, traffic flow dynamics, and other physical systems. Among these, the Korteweg–de Vries (KdV)-type equations have garnered significant attention due to their remarkable mathematical properties and physical relevance. These equations are particularly notable for admitting traveling wave solutions, known as solitary wave solutions, which are believed to effectively describe the soliton phenomenon first observed by Scott Russell in 1834. Furthermore, the KdV equation is widely recognized as a prototypical example of an exactly solvable equation. In recent years, several modified and generalized versions of the KdV equation have been introduced and extensively studied, driven by both physical applications and mathematical interest (Refs. 1–4 and references therein).

Considering the generalized KdV equation

$$u_t + (u^p)_x + u_{xxx} = 0, \quad (1)$$

it encompasses the classical KdV equation for  $p = 2$  and the modified KdV equation for  $p = 3$ . Notably, this equation is completely integrable for  $p = 2$  and  $p = 3$  but becomes nonintegrable for  $p = 4$ . Consequently, traditional methods, such as the inverse scattering transform, are not directly applicable to the quartic KdV equation, necessitating careful consideration of existence, uniqueness, stability, and asymptotic stability of solitons and collisions.<sup>5,6</sup> The generalized KdV equation (1) is derived from Euler's equation using the reductive perturbation method, where higher-order terms are truncated.

In addressing real-world problems, very often, it is essential to take truncated higher-order terms and other weakly dissipative influences into consideration. For instance, in modeling wave motions on a liquid layer over an inclined plane, Topper and Kawahara<sup>7</sup> derived the following system:

$$u_t + uu_x + u_{xxx} + \alpha u_{xx} + \gamma u_{xxxx} = 0. \quad (2)$$

Under conditions of a long inclined plane and weak surface tension, the diffusion term  $u_{xx}$  and the fourth-order dispersion term  $u_{xxxx}$  become negligible, leading to the perturbed KdV equation, as discussed in<sup>8</sup>

$$u_t + uu_x + u_{xxx} + \varepsilon(u_{xx} + u_{xxxx}) = 0, \quad (3)$$

where  $\varepsilon$  is a small positive perturbation parameter. This equation, known as the KdV equation with Kuramoto–Sivashinsky perturbation, loses its integrability due to the dissipative terms, making traditional methods, such as the Lax Pair method inapplicable for deriving solitary and periodic waves. Nonetheless, the existence and uniqueness of periodic waves for (3) have been explored in Refs. 8 and 9. For the modified KdV equation with the Kuramoto–Sivashinsky dissipation,

$$u_t + u^2 u_x + u_{xxx} + \varepsilon(u_{xx} + u_{xxxx}) = 0, \quad (4)$$

the existence of solitary waves was established in Ref. 10, while periodic traveling waves were derived using the Picard–Fuchs equation method, a tool from algebraic geometry.<sup>11</sup>

When two fluids with distinct surface tensions come into contact, or when a temperature gradient exists within a single fluid (e.g., when a liquid layer is heated from the air side), a tangential force arises along the interface, resulting in fluid flow. This flow is driven by the surface tension gradient, where the fluid with lower surface tension pulls the fluid with higher surface tension toward it. This phenomenon is referred to as the Marangoni effect or Marangoni convection.<sup>12</sup> Velarde<sup>12</sup> analyzed the steady heating of a liquid layer from the air side under the framework of the one-way long-wave approximation and derived the following governing equation:

$$u_t + \lambda_1 uu_x + \lambda_3 u_{xxx} + \varepsilon(\lambda_2 u_{xx} + \lambda_4 u_{xxxx} + \lambda_5 (uu_x)_x) = 0, \quad (5)$$

where the nonlinear term  $(uu_x)_x$  accounts for the Marangoni effect.<sup>13</sup> The dissipative KdV equation (5) also governs wave evolution in a shallow liquid layer, particularly in scenarios involving the transfer of surface-active material across the surface<sup>14,15</sup> or in modeling internal waves under shear conditions.<sup>16,17</sup> The existence of solitary waves

in Eq. (5) was rigorously proven in Ref. 18 using a dynamical systems approach. The periodic wave train was numerically verified in Ref. 19 and rigorously proven in Ref. 20, demonstrating the persistence of a unique periodic traveling wave under local dissipations. Mansour<sup>10</sup> studied a modified KdV equation incorporating three dissipative terms,

$$u_t + \lambda_1 u^2 u_x + \lambda_3 u_{xxx} + \varepsilon(\lambda_2 u_{xx} + \lambda_4 u_{xxxx} + \lambda_5 (uu_x)_x) = 0, \quad (6)$$

proving that solitary waves persist under small dissipations. The existence of periodic waves was established in Ref. 20.

Dissipation can also arise from nonlocal nonlinearity present in shallow water models, as those demonstrated in Refs. 21–24. In 2023, the modified KdV equation with nonlocal dissipation and weak fourth-order dispersion was studied in Ref. 22,

$$u_t + (u^2(f * u))_x + u_{xxx} + \tau u_{xxxx} = 0, \quad (7)$$

where  $0 < \tau \ll 1$ , and  $f * u$  is a convolution defined as

$$(f * u)(x, t) = \int_{-\infty}^t f(t-s)u(x, ts) ds,$$

with  $f(t) = \frac{1}{\tau} e^{-\frac{t}{\tau}}$ ; it was proved that Eq. (7) has a solitary wave or a unique periodic wave under certain conditions.

**Remark 1.** The Kuramoto–Sivashinsky dissipation term  $u_{xx} + u_{xxxx}$  has also been incorporated into the generalized Benjamin–Bona–Mahony (BBM) equation, as reported in Refs. 25 and 27 as well as in the Camassa–Holm equation, as discussed in Ref. 28. Furthermore, nonlocal dissipation induced by convolution has been considered for the BBM equation in Refs. 23 and 24 and similarly for the Camassa–Holm equation in Ref. 21 and for the Degasperis–Procesi equation.<sup>29</sup> In these studies, the existence of solitary waves or a unique periodic traveling wave has been rigorously established.

In this paper, we focus on the critical quartic KdV equation with multiple dissipation mechanisms, specifically incorporating the Kuramoto–Sivashinsky dissipation and Marangoni convection. It is given by

$$u_t + u^3 u_x + u_{xxx} + \varepsilon(\lambda_1 u_{xx} + \lambda_2 (uu_x)_x + \lambda_3 u_{xxxx}) = 0, \quad (8)$$

where  $\varepsilon > 0$  is a sufficiently small parameter, and  $\lambda_1$ ,  $\lambda_2$ , and  $\lambda_3$  are treated as free parameters.

We demonstrate that the model considered in this work could potentially be applied to study scenarios where nonlinear wave propagation is affected by both intrinsic instabilities (KS dissipation) and interfacial flows driven by surface tension gradients (Marangoni convection). Our main interest lies in exploring the existence of solitary waves and periodic waves, and their dynamics.

Our main findings are summarized in the following theorem.

**Theorem 2.** Let  $\alpha_0 = -(\frac{\lambda_1}{4c} + \frac{\lambda_3}{4})$ ,  $\alpha_1 = -\frac{\lambda_2}{(4c)^{\frac{2}{3}}}$ ,  $\alpha_2 = \lambda_3$ , and  $c$  represent the traveling wave speed associated with Eq. (8). The following statements hold:

(i) **Solitary wave solutions:**

The equation admits a solitary wave solution if and only if the triplet  $(\alpha_0, \alpha_1, \alpha_2)$  lies on a surface in  $\mathbb{R}^3$ , which is perturbed by

a distance of  $O(\varepsilon)$  from the plane,

$$a^* \alpha_0 + \frac{10}{9} \alpha_1 + \frac{70a^*}{91} \alpha_2 = 0, \text{ where } a^* = \frac{3 \cdot 20^{\frac{2}{3}} \Gamma(\frac{2}{3}) \Gamma(\frac{5}{6})}{14\sqrt{\pi}}.$$

(ii) **Small-amplitude periodic waves:**

For any fixed wave speed  $c$ , there exist parameter values  $(\alpha_0, \alpha_1, \alpha_2)$  in a neighborhood of  $(\frac{\alpha_2}{2}, -\frac{3\alpha_2}{2}, \alpha_2)$ , with  $\alpha_2 \neq 0$ , such that Eq. (8) supports two small-amplitude periodic traveling waves. These waves emerge through a degenerate Hopf bifurcation near the homogeneous state.

(iii) **Large-amplitude periodic waves:**

For any fixed wave speed  $c$ , there exist parameter values  $(\alpha_0, \alpha_1, \alpha_2)$  such that Eq. (8) exhibits two periodic traveling waves of large amplitudes. These waves arise due to a degenerate homoclinic bifurcation.

(iv) **Maximum number of periodic waves:**

For any fixed wave speed  $c$  and any  $(\alpha_0, \alpha_1, \alpha_2) \in \mathbb{R}^3$ , Eq. (8) admits at most two periodic traveling waves, which originate from a Poincaré bifurcation.

(v) **Bifurcation diagram:**

When projected onto the plane  $\alpha_2 = 1$  in  $\mathbb{R}^3$  (see Fig. 1), the bifurcation diagram consists of three bifurcation lines that divide  $\alpha_2 = 1$  into five open regions,  $\mathcal{V}_i$ ,  $i = 1, 2, 3, 4, 5$ .

(v1) For  $(\alpha_0, \alpha_1) \in \mathcal{V}_3 \cup \mathcal{V}_4$ , Eq. (8) has no periodic traveling waves.

(v2) For  $(\alpha_0, \alpha_1) \in \mathcal{V}_1 \cup \mathcal{V}_2$ , Eq. (8) admits exactly one periodic traveling wave.

(v3) For  $(\alpha_0, \alpha_1) \in \mathcal{V}_5$ , Eq. (8) admits two periodic traveling waves.

(v4) For  $(\alpha_0, \alpha_1)$  located in the line segment between  $D_2$  and  $D_3$ , Eq. (8) admits a solitary wave and a periodic wave.

We demonstrate that, in contrast to the unique existence of a periodic traveling wave previously derived in Refs. 11, 20, and 23–26 for the KdV-like equation, our study reveals the presence of two distinct periodic traveling waves. These waves differ in amplitude but share the same wave speed. Our studies also show the coexistence of a solitary wave and a periodic wave. To uncover these solutions, we employ a variety of analytical mechanisms, including a degenerate Hopf bifurcation, a homoclinic bifurcation, and a Poincaré bifurcation. In previous studies, the primary approach relied on analyzing the zeros of an Abelian integral by ensuring monotonicity in the ratio of its constituent elements, which effectively established the uniqueness of the zero. However, when these techniques are applied to Eq. (8), they prove inadequate due to the complex interplay of multiple dissipative terms, particularly those associated with Kuramoto–Sivashinsky dissipation and Marangoni convection. These dissipative effects introduce three fundamental components into the Abelian integrals, whose intricate coupling gives rise to multiple zeros, significantly complicating their determination. Estimating the number of zeros of an Abelian integral is closely related to the weak Hilbert’s 16th problem.<sup>32</sup>

Furthermore, the heightened nonlinearity inherent in the Hamiltonian, where the unperturbed Korteweg–de Vries (KdV) equation has a polynomial degree of five—compounds the complexity, as the associated Picard–Fuchs equation takes on a four-dimensional structure. Traditional analytical methods are

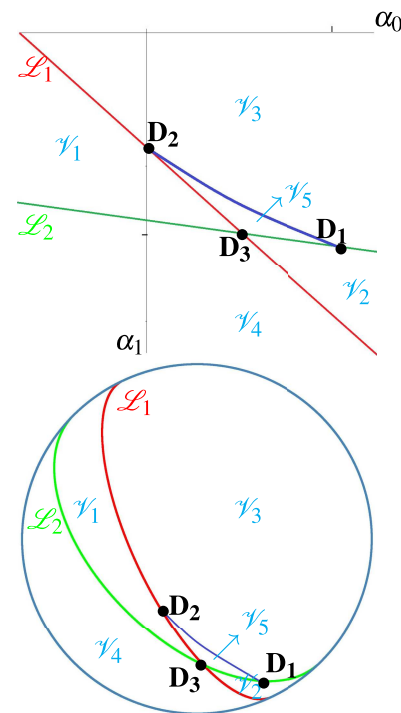


**FIG. 1.** Bifurcation diagram for the equation (8). More precisely, the top graph shows the bifurcation diagram projected on the plane  $\alpha_2 = 1$ , while the bottom one shows the bifurcation diagram projected on the Poincaré disk.  $\mathcal{L}_1 : a^* \alpha_0 + \frac{10}{9} \alpha_1 + \frac{70a^*}{91} = 0$  represents the homoclinic bifurcation line,  $\mathcal{L}_2 : \alpha_0 + \alpha_1 + 1 = 0$  is the Hopf bifurcation line, and the curve connecting  $D_1$  at  $(\frac{1}{2}, -\frac{3}{2})$  and  $D_2$  at  $(0, -\frac{63a^*}{91})$  indicates the saddle-node bifurcation of limit cycles,  $D_1$  is the degenerate Hopf bifurcation point,  $D_2$  is the degenerate homoclinic bifurcation point, and  $D_3$  at  $(\frac{10(13-9a^*)}{13(9a^*-10)}, \frac{27a^*}{13(10-9a^*)})$  is the Hopf-homoclinic bifurcation point.

insufficient to handle this complexity, necessitating alternative approaches. Of particular interest is the Abelian integral (23) defined on a normally hyperbolic manifold, which we examine in Secs. II–IV, while this integral shares the same expression as that employed in the classical study<sup>30</sup> on codimension-three Bogdanov–Takens (BT) bifurcation. The Picard–Fuchs equation approach used in Ref. 30 is not directly applicable to the Abelian integral (23) in our framework.

The remainder of this paper is organized as follows: Sec. II introduces bifurcation theory for near-Hamiltonian systems in the context of the weak Hilbert’s 16th problem, alongside preliminary lemmas. We then transform the infinite-dimensional dynamical system represented by the PDE model (8) into a finite-dynamical system, resulting in a regular perturbation problem on a normally hyperbolic invariant manifold. In Sec. III, we prove the existence of a solitary wave and derive asymptotic expansions for the Abelian integral, a critical tool for investigating a degenerate Hopf bifurcation and a homoclinic bifurcation on the normally hyperbolic manifold.

Subsequently, we establish the fourth assertion of Theorem 2. Section IV validates the fifth assertion of Theorem 2 and constructs the corresponding bifurcation diagram.

## II. MECHANISMS OF BURSTING PERIODIC TRAVELING WAVES

In this section, we introduce three mechanisms for bursting periodic traveling waves utilizing the bifurcation theory of near-Hamiltonian systems. Subsequently, we reduce the infinite-dimensional dynamical systems of the partial differential equation (PDE) (8) into a finite-dimensional dynamical system. More precisely, we derive a near-Hamiltonian system on a normally hyperbolic two-dimensional invariant manifold.

We briefly outline three mechanisms of bursting periodic orbits (limit cycles) in near-Hamiltonian systems, which correspond to periodic traveling waves in our framework.

### A. Three mechanisms of bursting periodic traveling waves and the weak Hilbert's 16th problem in near-Hamiltonian systems

We consider a polynomial near-Hamiltonian system given by

$$\dot{x} = H_y(x, y) + \varepsilon p(x, y, \varepsilon), \quad \dot{y} = -H_x(x, y) + \varepsilon q(x, y, \varepsilon). \quad (9)$$

Assuming that the unperturbed system (9) <sub>$\varepsilon=0$</sub>  possesses a family of clockwise closed orbits  $\{L_h\} = \{(x, y) : H(x, y) = h, h_c < h < h_\dagger\}$ , surrounding a center  $L_{h_c}$  located at  $(x_c, y_c)$  (with  $H(x_c, y_c) = h_c$ ) and bounded by a homoclinic loop  $L_{h_\dagger}$  [defined by  $H(x, y) = h_\dagger$ ]. Under the perturbation, the periodic structure is disrupted, with the center potentially transforming into a weak focus, the homoclinic loop and periodic orbits breaking, and only a finite number of isolated periodic orbits (limit cycles) persisting. These persisting limit cycles are located near the center, near the homoclinic loop, or distributed within the period annulus  $\{L_h\}$ . The associated three mechanisms of bursting limit cycles are known as a degenerate Hopf bifurcation, a homoclinic bifurcation, and a Poincaré bifurcation, respectively. To study the three mechanisms, a displacement map can be constructed on the period annulus  $\{L_h\}$  (see Refs. 31 and 32). Let  $(\rho(h), 0)$  be the intersection of  $L_h$  with the positive  $u$  axis,  $T$  the period of  $L_h$ ,  $L_{h,\varepsilon}$  be the positive orbit of (20) starting from  $(\rho(h), 0)$  at time  $t = 0$ , and its first intersection point with the positive  $u$  axis at time  $t = T(\varepsilon)$  is denoted by  $(\pi(h, \varepsilon), 0)$ . Therefore, the difference between these two points can be measured as

$$\begin{aligned} d(h, \delta) &= H(\pi(h, \varepsilon), 0) - H(\rho(h), 0) \\ &= \int_{L_{h,\varepsilon}} dH \\ &= \int_{L_{h,\varepsilon}} [H_x(x, y)(H_y(x, y) + \varepsilon p(x, y, \varepsilon)) \\ &\quad + H_y(x, y)(-H_x(x, y) + \varepsilon q(x, y, \varepsilon))] dt \\ &= \varepsilon \int_0^{T(\varepsilon)} [q(x, y, \varepsilon)H_y(x, y) + p(x, y, \varepsilon)H_x(x, y)] dt \\ &= \varepsilon F(h, \delta, \varepsilon), \end{aligned}$$

where the vector  $\delta \in \mathbb{R}^m$  represents the coefficients of  $p(x, y, \varepsilon)$  and  $q(x, y, \varepsilon)$ . From the continuity theorem, one has

$$\lim_{\varepsilon \rightarrow 0} L_{h,\varepsilon} = L_h, \quad \lim_{\varepsilon \rightarrow 0} \pi(h, \varepsilon) = \rho(h), \quad \lim_{\varepsilon \rightarrow 0} T(\varepsilon) = T.$$

Consequently,  $F(h, \delta, \varepsilon) \rightarrow M(h, \delta)$  as  $\varepsilon \rightarrow 0$ , leading to  $d(h, \delta) = \varepsilon M(h, \delta) + O(\varepsilon^2)$ , where

$$M(h, \delta) = \oint_{L_h} q(x, y, 0) dx - p(x, y, 0) dy,$$

which is known as the Melnikov function or the Abelian integral for the near-Hamiltonian system (9). The weak Hilbert's 16th problem inquires about the maximal number of zeros of  $M(h, \delta)$  for a given  $n$ th-degree system (9), and it is fully resolved only for quadratic near-Hamiltonian systems (see Ref. 32).

For sufficiently small  $\varepsilon$ , the zeros of  $M(h, \delta)$  provide the zeros of  $d(h, \delta)$  by an implicit function theorem, thereby yielding limit cycles of system (9). The following theorem summarizes the relationship between the zeros of  $M(h, \delta)$  and limit cycles of the system (9).

**Theorem 3 (Poincaré–Pontrjagin–Andronov theorem,<sup>31,32</sup>).** For the system (9), one has

1. If  $M(h, \delta) = 0$  and  $M'(h, \delta) \neq 0$ , then there exists a hyperbolic limit cycle  $\tilde{L}_h$  of the system (9) such that  $\tilde{L}_h \rightarrow L_h$  as  $\varepsilon \rightarrow 0$ .
2. If  $M(h, \delta) = M'(h, \delta) = M''(h, \delta) = \dots = M^{(k-1)}(h, \delta) = 0$  and  $M^{(k)}(h, \delta) \neq 0$ , then the system (9) has at most  $k$  limit cycles for sufficiently small  $\varepsilon$  in the vicinity of  $L_h$ .
3. The total number of isolated zeros of  $M(h, \delta)$  (taking into account of their multiplicity) is an upper bound on the number of limit cycles of the system (9) that bifurcate from the annulus  $\{L_h\}$ .

We demonstrate that when the homoclinic loop  $L_{h_\dagger}$  connects a hyperbolic saddle and  $L_{h_c}$  is an elementary center,  $d(h, \delta)$  can be extended on the boundaries of  $\{L_h\}$ . Furthermore,

- (i) Zeros of  $M(h, \delta)$  located in a very small interval  $[h_c, h_c + \varepsilon_1]$  reveal limit cycles bursting by a degenerate Hopf bifurcation from the center  $(x_c, y_c)$ .
- (ii) Zeros in a very small interval  $(h_\dagger - \varepsilon_2, h_\dagger]$  reveal the limit cycles emerging via a homoclinic bifurcation except for the alien limit cycles, where  $\varepsilon_1$  and  $\varepsilon_2$  are positive and sufficiently small.
- (iii) Zeros in a compact subset of  $(h_c, h_\dagger)$  characterize limit cycles of system (9) by a Poincaré bifurcation.

The degenerate Hopf bifurcation and the homoclinic bifurcation can be studied by locating zeros from the asymptotic expansions of  $M(h, \delta)$  at  $h = h_c$  and  $h = h_\dagger$ , in the related small intervals  $[h_c, h_c + \varepsilon_1]$  and  $(h_\dagger - \varepsilon_2, h_\dagger]$ , respectively (see Ref. 31). Specifically, the persistence of the homoclinic loop  $L_{h_\dagger}$  is ensured by the following theorem.

**Theorem 4 (Persistence of the homoclinic loop<sup>31</sup>).** Let  $M(h_\dagger, \delta_\dagger) = 0$  for some  $\delta = \delta_\dagger$ . If  $\frac{\partial M(h_\dagger, \delta)}{\partial \delta}|_{\delta=\delta_\dagger} \neq 0$ , then there exist a neighborhood  $U$  of  $L_{h_\dagger}$ , a sufficiently small parameter  $\varepsilon_\dagger$ , and a differentiable function  $\delta^*(\varepsilon) = \delta_\dagger + O(\varepsilon)$  such that for  $0 < |\varepsilon| < \varepsilon_\dagger$  and  $\|\delta - \delta_\dagger\| < \varepsilon_\dagger$ , system (9) has a homoclinic loop if and only if  $\delta = \delta(\varepsilon)$ .



## B. Chebyshev criterion

In this subsection, we introduce a criterion that bounds the maximum number of zeros of the function  $M(h, \delta)$  within a global interval  $(h_c, h_\tau)$  for a specific class of Hamiltonian systems. This criterion serves as a valuable tool in proving certain aspects of our main results.

**Definition 5.** Let  $l_0(x), l_1(x), \dots, l_{m-2}(x)$  and  $l_{m-1}(x)$  be analytic functions well defined on a real open interval  $\mathcal{J}$ .

1. The continuous Wronskian of  $\{l_0(x), l_1(x), \dots, l_{i-1}(x)\}$  for  $x \in \mathcal{J}$  is

$$W[l_0(x), l_1(x), \dots, l_{i-1}(x)] = \begin{vmatrix} l_0(x) & l_1(x) & \cdots & l_{i-1}(x) \\ l'_0(x) & l'_1(x) & \cdots & l'_{i-1}(x) \\ \vdots & \vdots & \ddots & \vdots \\ l_0^{(i-1)}(x) & l_1^{(i-1)}(x) & \cdots & l_{i-1}^{(i-1)}(x) \end{vmatrix},$$

where  $l_i^{(j)}(x)$  is the  $j$ th order derivative of  $l_i(x)$ ,  $j \geq 2$ .

2. The set  $\{l_0(x), l_1(x), \dots, l_{m-1}(x)\}$  is called a Chebyshev system if any nontrivial linear combination,

$$\kappa_0 l_0(x) + \kappa_1 l_1(x) + \cdots + \kappa_{m-1} l_{m-1}(x),$$

has at most  $m - 1$  isolated zeros on  $\mathcal{J}$ .

3. The ordered set  $\{l_0(x), l_1(x), \dots, l_{m-1}(x)\}$  is termed an extended complete Chebyshev system (ECT-system) if for each  $i \in \{1, 2, \dots, m\}$  any nontrivial linear combination,

$$\kappa_0 l_0(x) + \kappa_1 l_1(x) + \cdots + \kappa_{i-1} l_{i-1}(x),$$

has at most  $i - 1$  zeros with multiplicities accounted.

Let  $H(x, y) = \mathbb{U}(x) + \frac{y^2}{2}$  be an analytic function with the center of the period annulus  $\{L_h\}$  located at the origin. The projection of  $\{L_h\}$  onto the  $x$  axis forms an interval  $(x_l, x_r)$  with  $x_l < 0 < x_r$ , and  $x\mathbb{U}'(x) > 0$  for all  $x \in (x_l, x_r) \setminus \{0\}$ . The equality  $\mathbb{U}(x) = \mathbb{U}(z(x))$  defines an analytic involution  $z = z(x)$  for all  $x \in (x_l, x_r)$ . Define

$$\mathbb{I}_i(h) = \oint_{\Gamma_h} \eta_i(x) y^{2s-1} dx \text{ for } h \in (0, h^*), \quad (10)$$

where  $s \in \mathbb{N}$  and  $\eta_i(x)$  are analytic functions on  $(x_l, x_r)$ ,  $i = 0, 1, \dots, m - 1$ . Furthermore, let

$$l_i(x) := \frac{\eta_i(x)}{\mathbb{U}'(x)} - \frac{\eta_i(z(x))}{\mathbb{U}'(z(x))}. \quad (11)$$

The following lemma, adapted from Ref. 33, establishes a crucial connection.

**Lemma 6 (Ref. 33).** Consider the integrals defined in (10) and the functions in (11). If  $s > m - 2$  and  $\{l_0, l_1, \dots, l_{m-1}\}$  is an ECT system on  $(x_l, 0)$  or  $(0, x_r)$ , then  $\{\mathbb{I}_0, \mathbb{I}_1, \dots, \mathbb{I}_{m-1}\}$  is an ECT system on  $(0, h^*)$ .

## C. Transformation from an infinite-dimensional dynamical system of Eq. (8) into a finite-dimensional one

In this subsection, we transform the infinite-dimensional dynamical system described by the partial differential equation

(PDE) (8) into a finite-dimensional dynamical system incorporating a singular perturbation. Subsequently, we reduce this finite-dimensional system to a near-Hamiltonian system confined to a two-dimensional invariant manifold. To achieve this, we introduce the moving coordinate frame  $\xi = x - ct$  into Eq. (8), resulting in

$$-c \frac{du}{d\xi} + u^3 \frac{du}{d\xi} + \frac{d^3 u}{d\xi^3} + \varepsilon \left( \lambda_1 \frac{d^2 u}{d\xi^2} + \lambda_2 \frac{d}{d\xi} \left( u \frac{du}{d\xi} \right) + \lambda_3 \frac{d^4 u}{d\xi^4} \right) = 0. \quad (12)$$

By integrating (12) once, we obtain the third-order ordinary differential equation (ODE) with a singular perturbation,

$$-cu + \frac{1}{4}u^4 + \frac{d^2 u}{d\xi^2} + \varepsilon \left( \lambda_1 \frac{du}{d\xi} + \lambda_2 u \frac{du}{d\xi} + \lambda_3 \frac{d^3 u}{d\xi^3} \right) = 0. \quad (13)$$

This equation can be reformulated as a three-dimensional dynamical system by introducing the variables  $v = \frac{du}{d\xi}$  and  $w = \frac{dv}{d\xi}$ ,

$$\begin{aligned} \frac{du}{d\xi} &= v, & \frac{dv}{d\xi} &= w, \\ \varepsilon \lambda_3 \frac{dw}{d\xi} &= cu - \frac{1}{4}u^4 - w - \varepsilon \lambda_1 v - \varepsilon \lambda_2 uv. \end{aligned} \quad (14)$$

We can introduce the time rescaling  $\xi = \varepsilon \zeta$  to Eq. (14) and obtain

$$\begin{aligned} \frac{du}{d\zeta} &= \varepsilon v, & \frac{dv}{d\zeta} &= \varepsilon w, \\ \lambda_3 \frac{dw}{d\zeta} &= cu - \frac{1}{4}u^4 - w - \varepsilon \lambda_1 v - \varepsilon \lambda_2 uv. \end{aligned} \quad (15)$$

It is known that the system (14) is referred to as the slow system, while the system (15) is a fast system. As  $\varepsilon \rightarrow 0$ , we have the so-called limiting slow system,

$$\frac{du}{d\xi} = v, \quad \frac{dv}{d\xi} = w, \quad 0 = cu - \frac{1}{4}u^4 - w, \quad (16)$$

and the limiting fast system,

$$\frac{du}{d\zeta} = 0, \quad \frac{dv}{d\zeta} = 0, \quad \frac{dw}{d\zeta} = cu - \frac{1}{4}u^4 - w. \quad (17)$$

Obviously, the dynamics of the system (16) are constrained to a manifold, usually referred to as the critical manifold of the system (16), which is defined by the resulting algebraic equation in (16); that is,

$$\mathcal{W}_0 = \left\{ (u, v, w) \in \mathbb{R}^3 : cu - \frac{1}{4}u^4 - w = 0 \right\}. \quad (18)$$

Note that the set  $\mathcal{W}_0$  is exactly the equilibrium set of the system (17). The following result can be established.

**Lemma 7.** The critical manifold  $\mathcal{W}_0$  defined in (18) is normally hyperbolic.

*Proof.* The critical manifold is precisely the set of equilibria of (17). The linearization of (17) at each point of  $(u, v, w) \in \mathcal{W}_0$  has two zero eigenvalues whose generalized eigenspace is the tangent space of the two-dimensional critical manifold  $\mathcal{W}_0$  of equilibria, and the other one eigenvalue is  $-1$ , whose eigenvector is not tangent to  $\mathcal{W}_0$ . Thus,  $\mathcal{W}_0$  is normally hyperbolic and attracting.  $\square$

From the discussion in Ref. 34, there exists a two-dimensional submanifold  $\mathcal{W}_\varepsilon$  within  $\mathbb{R}^3$ , lying within the Hausdorff distance of  $O(\varepsilon)$  from  $\mathcal{W}_0$ . To investigate periodic traveling waves of (8), we focus on periodic orbits of the ODE (15) residing on the invariant manifold  $\mathcal{W}_\varepsilon$ . We assume that  $\mathcal{W}_\varepsilon$  is governed by

$$\mathcal{W}_\varepsilon = \left\{ (u, v, w) \in \mathbb{R}^3 : w = cu - \frac{1}{4}u^4 + \varepsilon g(u, v, \varepsilon) \right\},$$

where  $g(u, v, w)$  admits an approximation:  $g(u, v, \varepsilon) = g_0(u, v) + \sum_{i=1}^{\infty} g_i(u, v)\varepsilon^i$ . Substituting this  $g(u, v, w)$  into the slow system (14), we have

$$\begin{aligned} \varepsilon \lambda_3 \left[ \varepsilon \frac{\partial g}{\partial u} v + \varepsilon \frac{\partial g}{\partial v} \left( cu - \frac{1}{4}u^4 + \varepsilon g \right) + (c - u^3)v \right] \\ = cu - \frac{1}{4}u^4 - \left( cu - \frac{1}{4}u^4 \right) + \varepsilon g(u, v, \varepsilon) - \varepsilon \lambda_2 uv - \lambda_1 v. \end{aligned} \quad (19)$$

Comparing the coefficients of  $\varepsilon$  in (19), we can determine  $g_0(u, v) = (-\lambda_1 + \lambda_3 c) - \lambda_2 u + \lambda_3 u^3$  and, therefore, project the system (14) onto  $\mathcal{W}_\varepsilon$ , yielding

$$\frac{du}{d\xi} = v,$$

$$\frac{dv}{d\xi} = cu - \frac{1}{4}u^4 + \varepsilon (-\lambda_1 + \lambda_3 c) - \lambda_2 u + \lambda_3 u^3 + O(\varepsilon^2).$$

For convenience in our later discussion, we introduce the scaling transformations  $u = \beta_1 \tilde{u}$ ,  $v = \beta_2 \tilde{v}$ ,  $\xi = \kappa \tilde{\xi}$ , and  $\tilde{\varepsilon} = 4c^{\frac{1}{2}}\varepsilon$ , where  $\beta_1 = (4c)^{\frac{1}{3}}$ ,  $\beta_2 = 4^{\frac{1}{3}}c^{\frac{5}{6}}$ , and  $\kappa = (c)^{-\frac{1}{2}}$  drop the tildes for simplicity and arrive at

$$\frac{du}{d\xi} = v, \quad (20)$$

$$\frac{dv}{d\xi} = u(1 - u^3) + \varepsilon (\alpha_0 + \alpha_1 u + \alpha_2 u^3) v + O(\varepsilon^2),$$

where

$$\alpha_0 = -\left(\frac{\lambda_1}{4c} + \frac{\lambda_3}{4}\right), \quad \alpha_1 = -\frac{\lambda_2}{(4c)^{\frac{2}{3}}}, \quad \alpha_2 = \lambda_3. \quad (21)$$

To analyze solitary waves and periodic traveling waves of (8), we focus on the persistent homoclinic loops and limit cycles of the traveling wave ODE system (20). As discussed above, this amounts to studying the zeros of an associated Abelian integral for the near-Hamiltonian system (20). The unperturbed system (20) <sub>$\varepsilon=0$</sub>  is a Hamiltonian system with the Hamiltonian given by

$$H(u, v) = \frac{v^2}{2} - \frac{u^2}{2} + \frac{u^5}{5}, \quad (22)$$

which governs the phase portraits by  $H(u, v) = h$ , as shown in Fig. 2. In particular,  $H(u, v) = 0$  defines the homoclinic loop  $\Gamma_0$  and a family of periodic orbits

$$\Gamma_h = \left\{ H(u, v) = h \in \left( -\frac{3}{10}, 0 \right) \right\}$$

surrounding an elementary center located at  $(1, 0)$  with  $H(1, 0) = -\frac{3}{10}$ . Correspondingly, the associated Abelian integral for the

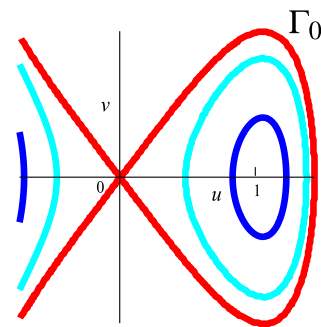


FIG. 2. The portraits of  $H(u, v) = h$ .

traveling wave ODE system (20) is given by

$$\mathcal{M}(h, \delta) = \oint_{\Gamma_h} (\alpha_0 + \alpha_1 u + \alpha_2 u^3) v du, \quad (23)$$

where  $\Gamma_h$  is defined on the normally hyperbolic manifold  $\mathcal{W}_\varepsilon$  with  $\delta = (\alpha_0, \alpha_1, \alpha_2) \in \mathbb{R}^3$ . The integrals  $\oint_{\Gamma_h} u^i v du$ , for  $i = 0, 1, 3$ , are referred to as the generating elements or generating Abelian integrals. It is noteworthy that the Abelian integral (23) shares the same form with the Abelian integral investigated in Ref. 30 for studying the codimension-three Bogdanov–Takens bifurcation of cusp type. However, the key difference lies in the context:  $\mathcal{M}(h, \delta)$  is defined within a normally hyperbolic manifold, with a higher-degree Hamiltonian given by (22), whereas the Abelian integral for the Bogdanov–Takens bifurcation utilizes a lower-degree Hamiltonian of the form  $H(u, v) = \frac{v^2}{2} - \frac{u^2}{2} + \frac{u^3}{3}$ . Despite the simplicity of the Hamiltonian (22), analyzing the zeros of  $\mathcal{M}(h, \delta)$  poses a significant challenge due to the increased dimensionality of the associated Picard–Fuchs equation, rendering the intersection analysis of the related functions particularly intricate. In Secs. III and IV, we delve into the local and global analysis of the zeros of  $\mathcal{M}(h, \delta)$ , aiming to uncover the number of periodic traveling waves arising from a degenerate bifurcation, a homoclinic bifurcation, and a Poincaré bifurcation.

### III. BURSTING PERIODIC TRAVELING WAVES VIA A DEGENERATE HOPF BIFURCATION AND A HOMOCLINIC BIFURCATION

#### A. Existence of a solitary wave

In this subsection, we rigorously establish the persistence of a homoclinic loop in the immediate vicinity of  $\Gamma_0$  within the framework of system (20). This endeavor serves to validate the claim (i) of Theorem 2, specifically confirming the endurance of a solitary wave in the dissipative KdV equation (8). To achieve this, we employ Theorem 4 to derive an algebraic constraint involving  $(\alpha_0, \alpha_1, \alpha_2)$  that ensures  $\mathcal{M}(h, \delta)$  vanishes at  $h = 0$ . Note that the loop  $\Gamma_0$  is characterized by  $H(u, v) = 0$  for  $0 < u \leq (\frac{5}{3})^{\frac{1}{3}}$ . Through a meticulous integration incorporating suitable variable transformations,

we obtain

$$\mathcal{M}(0, \delta) = a^* \alpha_0 + \frac{10}{9} \alpha_1 + \frac{70a^*}{91} \alpha_2,$$

where  $a^* = \frac{3 \cdot 20^{\frac{2}{3}} \Gamma(\frac{2}{3}) \Gamma(\frac{5}{6})}{14\sqrt{\pi}}$ . Furthermore,  $\frac{\partial \mathcal{M}(0, \delta)}{\partial(\alpha_0, \alpha_1, \alpha_2)}$  is non-zero, confirming its non-triviality. In accordance with Theorem 4, the homoclinic bifurcation set is the plane given by

$$a^* \alpha_0 + \frac{10}{9} \alpha_1 + \frac{70a^*}{91} \alpha_2 = 0 \text{ in } \mathbb{R}^3.$$

Critically, the persistence of the homoclinic loop with minimal deformation is contingent upon  $(\alpha_0, \alpha_1, \alpha_2)$  residing within a slightly distorted version of this plane, located within an  $O(\varepsilon)$  neighborhood. This precise characterization underscores the conditions necessary for the existence of solitary waves in Eq. (8).

## B. Degenerate Hopf bifurcation and a homoclinic bifurcation on the invariant manifold $\mathcal{M}_\varepsilon$

To investigate the small-amplitude periodic traveling waves of Eq. (8), we must delve into the zeros of  $\mathcal{M}(h, \delta)$  within a narrow interval  $(-\frac{3}{10}, -\frac{3}{10} + \varepsilon_1)$ . These zeros are intimately linked to the periodic traveling waves of Eq. (8) via the mechanism of a degenerate Hopf bifurcation. To achieve this goal, we require the asymptotic expansion of  $\mathcal{M}(h, \delta)$  within the specified interval.

Upon introducing  $\sigma = \sqrt{3}\xi$ ,  $u = \frac{\sqrt{3}}{3}\tilde{u} + 1$ , and  $v = y$  to the system (20), we obtain

$$\begin{aligned} \frac{d\tilde{u}}{d\sigma} &= y, \\ \frac{dy}{d\sigma} &= -\tilde{u} - \frac{2\sqrt{3}\tilde{u}^2}{3} - \frac{4\tilde{u}^3}{9} - \frac{\sqrt{3}\tilde{u}^4}{27} + \varepsilon \tilde{q}(\tilde{u}, y). \end{aligned} \quad (24)$$

Here,  $\tilde{q}(\tilde{u}, y) = (\tilde{\alpha}_0 + \tilde{\alpha}_1 \tilde{u} + \tilde{\alpha}_2 \tilde{u}^2 + \tilde{\alpha}_3 \tilde{u}^3)y$ , where

$$\begin{aligned} \tilde{\alpha}_0 &= \frac{\sqrt{3}}{3} \alpha_0 + \frac{\sqrt{3}}{3} \alpha_1 + \frac{\sqrt{3}}{3} \alpha_2, \quad \tilde{\alpha}_1 = \frac{1}{3} \alpha_1 + \alpha_2, \\ \tilde{\alpha}_2 &= \frac{\sqrt{3}}{3} \alpha_2, \quad \tilde{\alpha}_3 = \frac{1}{9} \alpha_2. \end{aligned}$$

The associated Hamiltonian takes the form

$$\tilde{H}(\tilde{z}, y) = \frac{y^2}{2} + \frac{\tilde{u}^2}{2} + \frac{2\sqrt{3}\tilde{u}^3}{9} + \frac{\tilde{u}^4}{9} + \frac{\sqrt{3}\tilde{u}^5}{135},$$

and the related Abelian integral is given by

$$\tilde{\mathcal{M}}^*(h, \delta) = \oint_{\Gamma_h} \tilde{q}(\tilde{u}, y) du = \sum_{i=0}^3 \tilde{\alpha}_i \oint_{\Gamma_h} \tilde{u}^i y d\tilde{u}. \quad (25)$$

Note that  $\mathcal{M}(h, \delta) = \tilde{\mathcal{M}}^*(h, \delta)$  according to Remark 3.1.4 of Ref. 31.

**Lemma 8.** For  $0 < h + \frac{3}{10} \ll 1$ , one has

$$\begin{aligned} \mathcal{M}(h, \delta) &= d_0 \left(h + \frac{3}{10}\right) + d_1 \left(h + \frac{3}{10}\right)^2 + d_2 \left(h + \frac{3}{10}\right)^3 \\ &\quad + O\left(\left(h + \frac{3}{10}\right)^4\right), \end{aligned}$$

where

$$\begin{aligned} d_0 &= \frac{2\sqrt{3}\pi}{3} (\alpha_0 + \alpha_1 + \alpha_2), \\ d_1 &= \frac{\sqrt{3}\pi}{27} (7\alpha_0 + \alpha_1 - 2\alpha_2), \\ d_2 &= \frac{\sqrt{3}\pi}{1458} (469\alpha_0 + 31\alpha_1 - 35\alpha_2). \end{aligned}$$

*Proof.* It suffices to study the asymptotic expansion of  $\tilde{\mathcal{M}}^*(h, \delta)$ . Let  $\Phi^*(\tilde{u}) = \tilde{H}(\tilde{u}, y) - \frac{y^2}{2}$  and define

$$\begin{aligned} \rho &= \phi(\tilde{u}) = \tilde{u} \left( \frac{2\Phi^*(\tilde{u})}{\tilde{u}^2} \right)^{\frac{1}{2}} \\ &= \tilde{u} \left( 1 + \frac{7\sqrt{2}}{6} \tilde{u} + \frac{9}{8} \tilde{u}^2 + \frac{\sqrt{2}}{4} \tilde{u}^3 + \frac{1}{24} \tilde{u}^4 \right)^{\frac{1}{2}}. \end{aligned}$$

Denote the left and right intersection points of the oval  $\Gamma_h$  with the  $\tilde{u}$  axis by  $(\tilde{u}_1(h), 0)$  and  $(\tilde{u}_2(h), 0)$ , respectively. Then,

$$\phi(\tilde{u}_1(h)) = -\left[2\left(h + \frac{3}{10}\right)\right]^{\frac{1}{2}}, \quad \phi(\tilde{u}_2(h)) = \left[2\left(h + \frac{3}{10}\right)\right]^{\frac{1}{2}}.$$

Furthermore,

$$\begin{aligned} \oint_{\Gamma_h} \tilde{u}^i y d\tilde{u} &= 2 \int_{\tilde{u}_1(h)}^{\tilde{u}_2(h)} \tilde{u}^i \sqrt{2\left(h + \frac{3}{10}\right) - 2\Phi^*(\tilde{u})} d\tilde{u} \\ &= 2\sqrt{2} \int_{\tilde{u}_1(h)}^{\tilde{u}_2(h)} \tilde{u}^i \sqrt{\left(h + \frac{3}{10}\right) - \frac{1}{2}\rho^2} d\tilde{u} \\ &= 2\sqrt{2} \int_{-\left[2\left(h + \frac{3}{10}\right)\right]^{\frac{1}{2}}}^{\left[2\left(h + \frac{3}{10}\right)\right]^{\frac{1}{2}}} \sqrt{\left(h + \frac{3}{10}\right) - \frac{1}{2}\rho^2} \frac{\tilde{u}^i}{\phi'(\tilde{u})} d\rho \\ &= 4\sqrt{2} \sum_{j \geq 0} r_{ij} I_{ij}(h), \end{aligned} \quad (26)$$

where  $i + j$  is even,

$$I_{ij}(h) = \int_0^{\left[2\left(h + \frac{3}{10}\right)\right]^{\frac{1}{2}}} \sqrt{\left(h + \frac{3}{10}\right) - \frac{1}{2}\rho^2} \rho^{i+j} d\rho,$$



and the coefficients  $r_{ij}$  can be computed as shown below,

$$\begin{aligned} r_{0,0} &= 1, r_{0,2} = \frac{7}{9}, r_{0,4} = \frac{469}{486}, r_{0,6} = \frac{217798}{164025}, \\ r_{1,1} &= -\frac{2\sqrt{3}}{3}, r_{1,3} = -\frac{73\sqrt{3}}{81}, r_{1,5} = -\frac{405\sqrt{3}}{518}, \\ r_{2,0} &= 1, r_{2,2} = \frac{55}{27}, r_{3,1} = -\frac{10\sqrt{3}}{9}, r_{3,3} = -\frac{931\sqrt{3}}{405}, \\ r_{4,0} &= 1. \end{aligned} \quad (27)$$

Introducing the transformation  $\bar{\rho} = \frac{\rho}{[2(h + \frac{1}{12})]^{\frac{1}{2}}}$ , we have

$$\begin{aligned} I_{ij}(h) &= 2^{\frac{i+j+1}{2}} \int_0^1 \sqrt{\left(h + \frac{3}{10}\right) - \left(h + \frac{3}{10}\right) \bar{\rho}^2} \bar{\rho}^2 \left(h + \frac{3}{10}\right)^{\frac{1}{2}} \\ &\times \bar{\rho}^{i+j} \left(h + \frac{3}{10}\right)^{\frac{i+j}{2}} d\bar{\rho} = \beta_{ij} \left(h + \frac{3}{10}\right)^{\frac{i+j}{2}+1}, \end{aligned} \quad (28)$$

where  $\beta_{ij} = 2^{\frac{i+j+1}{2}} \int_0^1 \sqrt{1 - \bar{\rho}^2} \bar{\rho}^{i+j} d\bar{\rho}$ . In particular,

$$\begin{aligned} \beta_{0,0} &= \frac{\sqrt{2}\pi}{4}, \beta_{0,2} = \beta_{1,1} = \beta_{2,0} = \frac{\sqrt{2}\pi}{8}, \\ \beta_{0,4} &= \beta_{1,3} = \beta_{2,2} = \beta_{3,1} = \beta_{4,0} = \frac{\sqrt{2}\pi}{8}, \\ \beta_{0,6} &= \beta_{1,5} = \beta_{2,4} = \beta_{3,3} = \beta_{4,2} = \frac{5\sqrt{2}\pi}{32}. \end{aligned}$$

Substituting (26)–(28) into (25) gives

$$\begin{aligned} M(h, \delta) &= M^*(h, \delta) \\ &= \sum_{i=0}^3 \tilde{\alpha}_i \oint_{\Gamma_h} \tilde{u}^i y d\tilde{u} = 4\sqrt{2} \sum_{i=0}^3 \tilde{\alpha}_i \left( \sum_{j \geq 0} r_{ij} I_{ij} \right) \\ &= 4\sqrt{2} \sum_{i=0}^3 \tilde{\alpha}_i \left( \sum_{j \geq 0} r_{ij} \beta_{ij} \left(h + \frac{3}{10}\right)^{\frac{i+j}{2}+1} \right) \\ &= \left(h + \frac{3}{10}\right) \sum_{l \geq 0} d_l \left(h + \frac{3}{10}\right)^l, \end{aligned}$$

where  $d_l = 4\sqrt{2} \sum_{i+j=l} \tilde{\alpha}_i r_{ij} \beta_{ij}$ ,  $l \in \mathbb{N}$ . Direct collecting  $r_{ij}$  for  $d_l$  completes the proof.  $\square$

To investigate the large-amplitude periodic traveling waves of Eq. (8), we focus on studying the zeros of the function  $\mathcal{M}(h, \delta)$  within a narrow interval  $(-\epsilon_2, 0)$ , where  $\epsilon_2$  is positive and sufficiently small. These zeros correspond to the periodic traveling waves of Eq. (8) through a homoclinic bifurcation. An efficient tool for this analysis is the asymptotic expansion of  $\mathcal{M}(h, \delta)$  near  $h = 0$  within a narrow interval  $(-\epsilon_2, 0)$ . Recall that for a general near-Hamiltonian system (9), near a homoclinic loop connecting a hyperbolic saddle, the Melnikov function  $M(h, \delta)$  can be expanded as  $M(h, \delta) = \sum_{j \geq 0} c_j (h^j + h \ln |h|)$  near a homoclinic loop connecting a hyperbolic saddle.<sup>31,35</sup> Specifically, the first four coefficients can be derived

using formulas presented in Theorem 2.2 of Ref. 35. Applying these formulas to our context, we obtain the following lemma:

**Lemma 9.** For  $0 < -h \ll 1$ ,

$$\mathcal{M}(h, \delta) = e_0 + e_1 h \ln(-h) + e_2 h + O(h^2 \ln(h)),$$

where

$$\begin{aligned} e_0 &= a^* \alpha_0 + b^* \alpha_1 + c^* \alpha_2, \quad e_1 = -\alpha_0, \\ e_2 &= d^* \alpha_1 + \frac{10}{3} \alpha_2, \end{aligned} \quad (29)$$

$$\begin{aligned} \text{with } a^* &= \frac{3 \cdot 20^{\frac{2}{3}} \Gamma(\frac{2}{3}) \Gamma(\frac{5}{6})}{14\sqrt{\pi}}, \quad b^* = \frac{10}{9}, \quad c^* = \frac{15 \cdot 20^{\frac{2}{3}} \Gamma(\frac{2}{3}) \Gamma(\frac{5}{6})}{91\sqrt{\pi}}, \\ d^* &= \frac{2\pi^{\frac{3}{2}} 20^{\frac{1}{3}} \sqrt{3}}{9\Gamma(\frac{2}{3}) \Gamma(\frac{5}{6})}. \end{aligned}$$

Using the asymptotic expansions of  $\mathcal{M}(h, \delta)$  in two narrow intervals, we proceed to prove the second and third claims of Theorem 2.

*Proof of (ii) and (iii) of Theorem 2.* We aim to show that there exist certain values of  $(\alpha_0, \alpha_1, \alpha_2)$  near specific points such that  $\mathcal{M}(h, \delta)$  has two zeros inside  $(-\epsilon_2, 0)$  or  $(-\frac{3}{10}, \epsilon_1 - \frac{3}{10})$ . We focus on proving the claim regarding values near  $(0, -\frac{c^* \alpha_2}{b^*}, \alpha_2)$  with  $\alpha_2 \neq 0$  such that  $\mathcal{M}(h, \delta)$  has two zeros inside  $(-\epsilon_2, 0)$ , emerging periodic traveling waves through a homoclinic bifurcation. The other case can be treated similarly.

First, consider the system of equations  $e_0 = e_1 = 0$ . For  $\alpha_2 \neq 0$ , this system has a unique solution  $(\alpha_0^*, \alpha_1^*, \alpha_2^*) = (0, -\frac{c^* \alpha_2}{b^*}, \alpha_2)$ . Without loss of generality, we set  $\alpha_2 = 1$ , leading to  $e_2 = \frac{10}{3} - \frac{c^* d^*}{b^*} < 0$  at  $(\alpha_0^*, \alpha_1^*, 1) = (0, -\frac{c^*}{b^*}, 1)$ . Additionally, the determinant of the Jacobian matrix  $\det \left| \frac{\partial(e_0, e_1)}{\partial(\alpha_0, \alpha_1)} \right| = \frac{10}{9} \neq 0$ , indicating that  $e_0$  and  $e_1$  can be treated as independent parameters.

We then choose the values of  $e_1$  and  $e_0$  in turns such that  $0 < e_0 \ll -e_1 \ll |\frac{10}{3} - \frac{c^* d^*}{b^*}|$ . This choice ensures that  $\mathcal{M}(h, \delta)$  has two zeros near  $h = 0$  within a very narrow interval  $(-\epsilon_2, 0)$ . Noting that  $e_0$  and  $|e_1|$  are taken to be sufficiently small, and then underground parameter  $(\alpha_0, \alpha_1, 1)$  must lie in a subset  $\mathcal{U}^*$  of a sufficiently small neighborhood  $\mathcal{U}$  of  $(\alpha_0^*, \alpha_1^*, 1)$ , where  $\mathcal{U}^* = \{(\alpha_0, \alpha_1, 1) : 0 < c_0 \ll -c_1 \ll \frac{c^* d^*}{b^*} - e^*\}$ . This completes the proof.  $\square$

### C. Bursting periodic traveling waves by a Poincaré bifurcation

To uncover the count of periodic traveling waves in Eq. (8) arising from a Poincaré bifurcation, the core problem is the precise bound on the maximal number of zeros of  $\mathcal{M}(h, \delta)$  within  $h \in (-\frac{3}{10}, 0)$ . We introduce  $u = \tilde{u} + 1$  to system (20) and arrive at

$$\begin{aligned} \dot{u} &= v, \\ \dot{v} &= -\tilde{u}(\tilde{u} + 1)(\tilde{u}^2 + 3\tilde{u} + 3) + \varepsilon(\alpha_0 + \alpha_1 + \alpha_2 \\ &\quad + (\alpha_1 + 3\alpha_2)\tilde{u} + \alpha_2(\tilde{u}^3 + 3\tilde{u}^2))v. \end{aligned} \quad (30)$$

The corresponding Hamiltonian and Abelian integrals are given by

$$\bar{H}(u, v) = -\frac{3}{10} + \frac{v^2}{2} + \frac{3\bar{u}^2}{2} + \bar{u}^4 + 2\bar{u}^3 + \frac{\bar{u}^5}{5} \doteq \frac{v^2}{2} + \Phi(\bar{u})$$

and

$$\bar{M}(h, \delta) = \bar{\alpha}_0 I_0(h) + \bar{\alpha}_1 I_1(h) + \bar{\alpha}_2 \mathcal{I}_2(h), \quad (31)$$

respectively. Here,  $\mathcal{I}_2(h) = I_3(h) + 3I_2(h)$ , where  $I_i(h) = \oint_{\Gamma_h} \bar{u}^i v d\bar{u}$  for  $i = 0, 1, 2, 3$ , and  $\bar{\alpha}_0 = \alpha_0 + \alpha_1 + \alpha_2$ ,  $\bar{\alpha}_1 = \alpha_1 + 3\alpha_2$ ,  $\bar{\alpha}_2 = \alpha_2$ . Notably,  $\mathcal{M}(h, \delta) = \bar{M}(h, \delta)$ .

**Lemma 10.** For  $i \in \mathbb{N}$ ,  $2hI_i(h) = \oint_{\Gamma_h} f_i(\bar{u})v^3 d\bar{u}$  for  $i \in \mathbb{N}$ , where  $f_i(\bar{u}) = \frac{f_i^*(\bar{u})}{15(\bar{u}+1)^2(\bar{u}^2+3\bar{u}+3)^2}$ , with

$$\begin{aligned} f_i^*(\bar{u}) = & \bar{u}^i (2\bar{u}\bar{u}^6 + 18\bar{u}\bar{u}^5 + 17\bar{u}^6 + 72\bar{u}\bar{u}^4 + 136\bar{u}^5 + 161\bar{u}\bar{u}^3 \\ & + 476\bar{u}^4 + 210\bar{u}\bar{u}^2 + 924\bar{u}^3 + 150\bar{u}\bar{u} + 1050\bar{u}^2 + 45i \\ & + 660\bar{u} + 180). \end{aligned}$$

*Proof.* Using the identity  $2\Phi(\bar{u}) + v^2 = 2h$  on each  $\Gamma_h$ , we have

$$\begin{aligned} 2hI_i(h) &= \oint_{\Gamma_h} (2\Phi(\bar{u}) + v^2)\bar{u}^i v d\bar{u} \\ &= \oint_{\Gamma_h} 2\Phi(\bar{u})\bar{u}^i v d\bar{u} + \oint_{\Gamma_h} \bar{u}^i v^3 d\bar{u}. \end{aligned} \quad (32)$$

By taking  $k = 1$ ,  $F(\bar{u}) = 2\bar{u}^i \Phi(\bar{u})$ , and applying Lemma 4.1 from Ref. 33, we obtain

$$\oint_{\Gamma_h} 2\Phi(\bar{u})\bar{u}^i v d\bar{u} = \oint_{\Gamma_h} G_i(\bar{u})v^3 d\bar{u}. \quad (33)$$

Substituting (33) into (32) completes the proof.  $\square$

Next, we introduce the functions

$$l_i(\bar{u}, z) = \left( \frac{f_i}{\Phi'} \right)(\bar{u}) - \left( \frac{f_i}{\Phi'} \right)(z(\bar{u})), \quad i = 0, 1$$

and

$$l_2(\bar{u}, z) = \left( \frac{f_3 + 3f_2}{\Phi'} \right)(\bar{u}) - \left( \frac{f_3 + 3f_2}{\Phi'} \right)(z(\bar{u}))$$

for  $(\bar{u}, z) \in (-1, 0) \times \left( 0, \frac{10\frac{1}{3}}{3} - \frac{10\frac{2}{3}}{6} - \frac{5}{3} \right) \doteq \Delta$  satisfying  $\Phi(\bar{u}) - \Phi(z) = \frac{x-z}{10} q(\bar{u}, z) = 0$ , where

$$\begin{aligned} q(\bar{u}, z) = & 2\bar{u}^4 + 2\bar{u}^3 z + 2\bar{u}^2 z^2 + 2xz^3 + 2z^4 \\ & + 10x^3 + 10\bar{u}^2 z + 10xz^2 + 10z^3 + 20\bar{u}^2 + 20xz \\ & + 20z^2 + 15x + 15z. \end{aligned} \quad (34)$$

We compute  $W[l_1]$ ,  $W[l_1, l_2]$ , and  $W[l_1, l_2, l_0]$ , the Wronskians of  $l_0$ ,  $l_1$ , and  $l_2$ , respectively, as follows:

$$\begin{aligned} W[l_1] &= \frac{(\bar{u} - z)w_1(\bar{u}, z)}{15(\bar{u} + 1)^3(z + 1)^3(\bar{u}^2 + 3\bar{u} + 3)^3(z^2 + 3z + 3)^3}, \\ W[l_1, l_2] &= \frac{(\bar{u} - z)^3 w_2(\bar{u}, z)}{225(z + 1)^4(\bar{u} + 1)^4(z^2 + 3z + 3)^5(\bar{u}^2 + 3\bar{u} + 3)^5 p_0(\bar{u}, z)}, \\ W[l_1, l_2, l_0] &= \frac{(\bar{u} - z)^6 w_3(\bar{u}, z)}{3375\bar{u}^3 z^3(z + 1)^5(\bar{u} + 1)^5(\bar{u}^2 + 3\bar{u} + 3)^7(z^2 + 3z + 3)^7 p_0^3(\bar{u}, z)}, \end{aligned}$$

where  $p_0(\bar{u}, z) = 2\bar{u}^3 + 4\bar{u}^2 z + 6\bar{u}z^2 + 8z^3 + 10\bar{u}^2 + 20\bar{u}z + 30z^2 + 20 + 40z + 15$ ,  $w_1(\bar{u}, z)$ ,  $w_2(\bar{u}, z)$ , and  $w_3(\bar{u}, z)$  are three symmetric bivariate polynomials with long expressions, they have degrees 14, 23, and 36, respectively [Explicit expressions for  $w_k(\bar{u}, z)$ ,  $k = 1, 2, 3$  are provided as a [supplementary material](#)]. We compute the resultant between  $q(\bar{u}, z)$  and  $p_0(\bar{u}, z)$  with respect to  $z$ , obtaining a polynomial, which has no zeros for  $\bar{u} \in (-1, 0)$  (by applying Sturm's theorem). This implies that  $p_0(\bar{u}, z)$  has no roots on  $\Delta$ . Therefore, the Wronskians are all well-defined.

*Proof of (iv) of Theorem 2.* We need to show that  $\mathcal{M}(h, \delta)$  has at most two zeros located in  $(-\frac{3}{10}, 0)$  for all  $(\alpha_0, \alpha_1, \alpha_2) \in \mathbb{R}^3$ . By utilizing Eq. (31) and the identity  $\mathcal{M}(h, \delta) = \bar{M}(h, \delta)$  in conjunction

with Lemma 10, it suffices to demonstrate that any linear combination of the integrals

$$\left\{ \oint_{\Gamma_h} f_0(\bar{u})v^3 d\bar{u}, \oint_{\Gamma_h} f_1(\bar{u})v^3 d\bar{u}, \oint_{\Gamma_h} (f_3(\bar{u}) + 3f_2(\bar{u}))v^3 d\bar{u} \right\}$$

has at most two zeros. To achieve this, we must investigate whether this set forms a Chebyshev system or not. Consequently, we employ Lemma 6 to verify whether the associated Wronskians vanish.

First, we compute the resultant between  $w_1(\bar{u}, z)$  and  $q(\bar{u}, z)$  with respect to  $z$ , yielding a polynomial that has no zeros for  $\bar{u} \in (-1, 0)$  (as proven by Sturm's theorem). This implies that

$w_1(\bar{u}, z)$  does not vanish on the domain  $\Delta$ . Next, by triangularizing the algebraic set  $[w_2(\bar{u}, z), q(\bar{u}, z)]$  and isolating the roots using the algorithm of the symbolic computation described in Ref. 36, we show that  $[w_2(\bar{u}, z), q(\bar{u}, z)]$  has no roots for  $(\bar{u}, z) \in \Delta$ . Therefore,  $W[l_1(\bar{u}), l_2(\bar{u})]$  does not vanish for  $\bar{u} \in (-1, 0)$ . Similarly, we can prove that  $W[l_1(\bar{u}), l_2(\bar{u}), l_0(\bar{u})]$  also does not vanish for  $\bar{u} \in (-1, 0)$ . Hence, the set of integrals forms a Chebyshev system, implying that  $\mathcal{M}(h, \delta)$  has at most two zeros for  $h \in (-\frac{3}{10}, 0)$ . This completes the proof.  $\square$

#### IV. BIFURCATION DIAGRAM

In this section, we derive the bifurcation diagram for the emergence of periodic traveling waves in the quartic KdV equation (8). Without loss of generality, we assume  $\alpha_2 = 1$  in (23). Then,  $\mathcal{M}(h, \delta) = \alpha_0 J_0(h) + \alpha_1 J_1(h) + J_3(h)$ , where  $J_i(h) = \oint_{\Gamma_h} u^i dv$  represents the generating Abelian integral along  $\Gamma_h$ . First, we have  $J_0(h) = \oint_{\Gamma_h} \frac{1}{v} du = \oint_{\Gamma_h} \frac{v}{v} d\xi = \int_0^{T(h)} d\tau = T(h) > 0$ , where  $T(h)$  is the period of  $\Gamma_h$ . As  $h \rightarrow -\frac{3}{10}$ , indicating  $v \rightarrow 0$ , we have  $J_0(-\frac{3}{10}) = \lim_{h \rightarrow -\frac{3}{10}} \oint_{\Gamma_h} v du = \lim_{h \rightarrow -\frac{3}{10}} \int_0^T v^2 d\xi = 0$ . Thus,  $J_0(h) > 0$  for  $h \in (-\frac{3}{10}, 0)$ . Consequently, the ratio of the generating Abelian integrals, defined as

$$\mathcal{X}(h) = \frac{\alpha_1 J_1(h) + J_3(h)}{J_0(h)}, \quad (35)$$

is well defined for  $h \in (-\frac{3}{10}, 0)$ . This allows us to express  $\mathcal{M}(h, \delta)$  as  $\mathcal{M}(h, \delta) = J_0(h)(\alpha_0 + \mathcal{X}(h))$ . Next, we establish the following lemma regarding the behavior of  $\mathcal{X}(h)$ .

**Lemma 11.** *The function  $\mathcal{X}(h)$  satisfies the following limits:*

1. 
$$\lim_{h \rightarrow -\frac{3}{10}} \mathcal{X}(h) = \alpha_1 + 1, \quad \lim_{h \rightarrow 0} \mathcal{X}(h) = \frac{b^*}{a^*} \alpha_1 + \frac{71}{90}.$$
2. 
$$\lim_{h \rightarrow -\frac{3}{10}} \mathcal{X}'(h) = -\frac{1}{3} \alpha_1 - \frac{1}{2},$$
  

$$\lim_{h \rightarrow 0} \mathcal{X}'(h) = \text{Sign} \left( -\frac{b^*}{a^*} \alpha_1 - \frac{c^*}{a^*} \right) \infty.$$

*Proof.* A straightforward computation shows that

$$\mathcal{X}'(h) = \frac{(\alpha_1 J_1'(h) + J_3'(h))J_0(h) - (\alpha_1 J_1(h) + J_3(h))J_0'(h)}{J_0^2(h)}.$$

Using the asymptotic expansions of  $\mathcal{M}(h, \delta)$  from Lemmas 8 and 9, we can derive the asymptotic expansions of  $J_i(h)$  and  $J_i'(h)$  at  $h = 0$  and  $h = -\frac{3}{10}$  for  $i = 0, 1, 3$ . This allows us to compute the limits of  $\mathcal{X}(h)$  and  $\mathcal{X}'(h)$  at the two endpoints  $h = -\frac{3}{10}$  and  $h = 0$ . Direct computations complete the proof.  $\square$

Furthermore, we analyze the monotonicity of  $\mathcal{X}(h)$  in the following lemma:

**Lemma 12.** *For  $h \in (-\frac{3}{10}, 0)$ , the function  $\mathcal{X}(h)$  exhibits the following behaviors:*

1. When  $\alpha_1 \in (-\infty, -\frac{3}{2}]$ ,  $\mathcal{X}(h)$  increases monotonically from  $(-\frac{3}{10}, \alpha_1 + 1)$  to the right endpoint  $(0, \frac{b^*}{a^*} \alpha_1 + \frac{c^*}{a^*})$ .

2. When  $\alpha_1 \in (-\frac{3}{2}, -\frac{c^*}{b^*})$ ,  $\mathcal{X}(h)$  decreases monotonically from  $(-\frac{3}{10}, \alpha_1 + 1)$  to a minimum point  $(h^*, \mathcal{X}(h^*))$  and then increases monotonically to the right endpoint  $(0, \frac{b^*}{a^*} \alpha_1 + \frac{c^*}{a^*})$ . In particular,  $\mathcal{X}(-\frac{3}{10}) < \mathcal{X}(0)$  when  $\alpha_1 \in (-\frac{3}{2}, -\frac{27a^*}{91(b^*-a^*)})$ ,  $\mathcal{X}(-\frac{3}{10}) = \mathcal{X}(0)$  when  $\alpha_1 = -\frac{27a^*}{91(b^*-a^*)}$ , and  $\mathcal{X}(-\frac{3}{10}) > \mathcal{X}(0)$  when  $\alpha_1 \in (-\frac{27a^*}{91(b^*-a^*)}, -\frac{c^*}{b^*})$ .
3. When  $\alpha_1 \in [-\frac{c^*}{b^*}, +\infty)$ ,  $\mathcal{X}(h)$  decreases monotonically from  $(-\frac{3}{10}, \alpha_1 + 1)$  to the right endpoint  $(0, \frac{b^*}{a^*} \alpha_1 + \frac{c^*}{a^*})$ .

*Proof.* From 2 of Lemma 11, we know that  $\mathcal{X}'(-\frac{3}{10}) > 0$ ,  $\mathcal{X}''(0) > 0$  when  $\alpha_1 \in (-\infty, -\frac{3}{2}]$ . This implies that  $\mathcal{X}'(h)$  may have  $2n$  zeros, where  $n \geq 0$ . If  $\mathcal{X}'(h)$  possesses two or more zeros, then there necessarily exists a suitable  $\alpha_0$  for which  $\mathcal{M}(h, \delta)$  has at least three zeros, taking into account the inequality  $\mathcal{X}(0) > \mathcal{X}(-\frac{3}{10})$ . This finding contradicts the conclusion drawn in the proof of part (iv) of Theorem 2, which states that  $\mathcal{M}(h, \delta)$  can have at most two zeros within the interval  $(-\frac{3}{10}, 0)$ . Consequently, it follows that  $\mathcal{X}'(h)$  is positive, implying that  $\mathcal{X}(h)$  is an increasing monotonically in  $(-\frac{3}{10}, 0)$ .

Noting that  $\mathcal{X}'(-\frac{3}{10}) \mathcal{X}''(0) < 0$  for  $\alpha_1 \in (-\frac{3}{2}, -\frac{c^*}{b^*})$ , we deduce that  $\mathcal{X}'(h)$  has  $2n + 1$  zeros ( $n \geq 0$ ). However, if  $\mathcal{X}'(h)$  has three or more zeros, there must exist special values of  $\alpha_0$  such that  $\mathcal{M}(h, \delta)$  has at least three zeros. This conflicts with the established conclusion that  $\mathcal{M}(h, \delta)$  has at most two zeros within the interval  $(-\frac{3}{10}, 0)$ . Therefore,  $\mathcal{X}'(h)$  has a unique zero, denoted by  $h^*$ . This implies that  $\mathcal{X}(h)$  decreases monotonically from  $(-\frac{3}{10}, \alpha_1 + 1)$  to a minimum point  $(h^*, \mathcal{X}(h^*))$  and then increases monotonically toward the right endpoint  $(0, \frac{b^*}{a^*} \alpha_1 + \frac{c^*}{a^*})$ . The inequalities regarding the values of  $\mathcal{X}(h)$  at these endpoints can be directly derived by comparing their respective values. The third claim of Lemma 12 can be proved similarly.  $\square$

Based on Lemma 12, which characterizes the behavior of  $\mathcal{X}(h)$ , we strategically select  $\alpha_0 = -\mathcal{X}(h^*)$  to ensure that  $\alpha_0 + \mathcal{X}(h)$  vanishes at  $h = h^*$ , thereby guaranteeing that  $\mathcal{M}(h, \delta)$  has a zero at  $h = h^*$ . Leveraging this insight, we delineate the lines, curves, and regions that compose the bifurcation diagram for periodic traveling waves of the quartic KdV equation (8). The detailed analysis is as follows:

1. For any  $\alpha_1 \in \mathbb{R}$ , setting  $\alpha_0 = -\mathcal{X}(0)$  results in  $\mathcal{M}(0, \delta) = 0$ , indicating the persistence of a solitary wave. The homoclinic bifurcation set is then characterized by  $a^* \alpha_0 + \frac{10}{9} \alpha_1 + \frac{71a^*}{90} \alpha_2 = 0$ .
2. For any  $\alpha_1 \in \mathbb{R}$ , setting  $\alpha_0 = -\mathcal{X}(-\frac{3}{10})$  leads to  $\mathcal{M}(-\frac{3}{10}, \delta) = 0$ , corresponding to the Hopf bifurcation plane, characterized by  $\alpha_0 + \alpha_1 + \alpha_2 = 0$ .
3. For  $\alpha_1 \in (-\infty, -\frac{3}{2})$ , choosing  $\alpha_0 \in (-\mathcal{X}(0), -\mathcal{X}(-\frac{3}{10}))$  yields a unique zero of  $\mathcal{M}(h, \delta)$ , signifying the existence of a unique periodic traveling wave of (8). Conversely, selecting  $\alpha_0$  outside this interval results in the absence of periodic traveling waves.

4. For  $\alpha_1 \in \left(-\frac{3}{2}, -\frac{c^*}{b^*}\right)$ , setting  $\alpha_0 = -\min \mathcal{X}(h)$  for  $h \in \left(-\frac{3}{10}, 0\right)$  defines the double limit cycle bifurcation curve. Specifically,  $\alpha_0 = -\mathcal{X}\left(-\frac{3}{10}\right)$  with  $\mathcal{X}'\left(-\frac{3}{10}\right) = 0$  gives the degenerate Hopf bifurcation point  $\left(\frac{1}{2}, -\frac{3}{2}\right)$ , while  $\alpha_0 = -\mathcal{X}(0)$  and  $\alpha_0 = 0$  correspond to the degenerate homoclinic bifurcation point  $\left(0, -\frac{c^*}{b^*}\right)$ .
5. For  $\alpha_1 \in \left(-\frac{3}{2}, -\frac{c^*}{b^*}\right)$ , if  $-\alpha_0$  lies between  $\min \mathcal{X}(h)$  and  $\min \left\{\mathcal{X}\left(-\frac{3}{10}\right), \mathcal{X}(0)\right\}$ ,  $\mathcal{M}(h, \delta)$  has two simple zeros in  $\left(-\frac{3}{10}, 0\right)$ , indicating the emergence of two periodic traveling waves. Alternatively, if  $-\alpha_0$  falls within  $\left(\min \left\{\mathcal{X}\left(-\frac{3}{10}\right), \mathcal{X}(0)\right\}, \max \left\{\mathcal{X}\left(-\frac{3}{10}\right), \mathcal{X}(0)\right\}\right)$ ,  $\mathcal{M}(h, \delta)$  has a unique simple zero, ensuring the existence of a single periodic traveling wave. Choosing  $\alpha_0$  outside these intervals results in the absence of periodic traveling waves.
6. For  $\alpha_1 \in \left(-\frac{27a^*}{91(b^*-a^*)}, -\frac{c^*}{b^*}\right)$ , setting  $\alpha_0 = -\mathcal{X}(0)$  ensures  $\mathcal{M}(0, \delta) = 0$  and  $\mathcal{M}(h, \delta)$  has another zero in  $\left(-\frac{3}{10}, 0\right)$ , implying the coexistence of a solitary wave and a periodic wave.
7. For  $\alpha_1 \in \left(-\frac{c^*}{b^*}, +\infty\right)$ , selecting  $\alpha_0 \in \left(-\mathcal{X}\left(-\frac{3}{10}\right), -\mathcal{X}(0)\right)$  yields a unique zero of  $\mathcal{M}(h, \delta)$ , corresponding to a unique periodic traveling wave of Eq. (8). Conversely, choosing  $\alpha_0$  outside this interval results in the absence of periodic traveling waves.

Summarizing these findings, we can derive the bifurcation diagram provided in Fig. 1 and validate the last claim of Theorem 2.

## SUPPLEMENTARY MATERIAL

See the [supplementary material](#) that provides explicit expressions of three symmetric bivariate polynomials  $w_1(\bar{u}, z)$ ,  $w_2(\bar{u}, z)$ , and  $w_3(\bar{u}, z)$  with degrees 14, 23, and 36, respectively. These polynomials appear in the proof of Lemma 10.

## ACKNOWLEDGMENTS

This work was partially supported by the National Natural Science Foundation of China (No. 12471157), the Natural Science Foundation of Guangxi (No. 2020JG110003), and the Simons Foundation of USA (No. 628308).

## AUTHOR DECLARATIONS

### Conflict of Interest

The authors have no conflicts to disclose.

## Author Contributions

**Xianbo Sun:** Conceptualization (equal); Formal analysis (equal); Funding acquisition (equal); Methodology (equal); Writing – original draft (equal). **Mingji Zhang:** Conceptualization (equal); Formal analysis (equal); Funding acquisition (equal); Writing – review & editing (equal).

## DATA AVAILABILITY

The data that support the findings of this study are available within the article.

## REFERENCES

- <sup>1</sup>E. G. Shurgalina and E. N. Pelinovskaya, “Nonlinear dynamics of a soliton gas: Modified Korteweg–de Vries equation framework,” *Phys. Lett. A* **380**, 2049–2053 (2016).
- <sup>2</sup>J. A. Gear and R. Grimshaw, “A second-order theory for solitary waves in shallow fluids,” *Phys. Fluids* **26**, 14–29 (1983).
- <sup>3</sup>N. F. Smyth and A. L. Worthy, “Solitary wave evolution for mKdV equations,” *Wave Motion* **21**, 263–275 (1995).
- <sup>4</sup>L. Zhang, M. Han, M. Zhang, and C. M. Khalique, “A new type of solitary wave solution of the mKdV equation under singular perturbations,” *Int. J. Bifurc. Chaos* **30**, 2050162 (2020).
- <sup>5</sup>Y. Martel and F. Merle, “Inelastic interaction of nearly equal solitons for the quartic gKdV equation,” *Invent. Math.* **183**(3), 563–648 (2011).
- <sup>6</sup>Y. Martel and F. Merle, “Description of two soliton collision for the quartic gKdV equation,” *Ann. Math.* **174**, 757–857 (2011).
- <sup>7</sup>J. Topper and T. Kawahara, “Approximate equations for long nonlinear waves on a viscous fluid,” *J. Phys. Soc. Jpn.* **44**, 663–666 (1978).
- <sup>8</sup>T. Ogawa, “Travelling wave solutions to a perturbed Korteweg–de Vries equation,” *Hiroshima J. Math.* **24**, 401–422 (1994).
- <sup>9</sup>G. Derks and S. Gils, “On the uniqueness of traveling waves in perturbed Korteweg–de Vries equations,” *Jpn. J. Ind. Appl. Math.* **10**, 413–430 (1993).
- <sup>10</sup>M. B. A. Mansour, “A geometric construction of traveling waves in a generalized nonlinear dispersive-dissipative equation,” *J. Geom. Phys.* **69**, 116–122 (2013).
- <sup>11</sup>A. Chen, L. Guo, and W. Huang, “Existence of kink waves and periodic waves for a perturbed defocusing mKdV equation,” *Qual. Theory Dyn. Syst.* **17**, 495–517 (2018).
- <sup>12</sup>M. G. Velarde, *Physicochemical Hydrodynamics: Interfacial Phenomena* (Plenum, New York, 1987).
- <sup>13</sup>P. L. Garcia-Ybarra, J. L. Castillo, and M. G. Velarde, “Bénard-Marangoni convection with a deformable interface and poorly conducting boundaries,” *Phys. Fluids* **30**, 2655–2661 (1987).
- <sup>14</sup>M. G. Velarde and X. L. Chu, “The harmonic oscillator approach to sustained gravity-capillary (Laplace) waves at liquid interfaces,” *Phys. Lett. A* **131**, 430–432 (1988).
- <sup>15</sup>M. G. Velarde, A. A. Nepomnyashchy, and M. Hennenberg, “Onset of oscillatory interfacial instability and wave motions in Bénard layers,” in *Advances in Applied Mechanics* (Elsevier, 2001), Vol. 37, pp. 167–238.
- <sup>16</sup>P. D. Weidman and M. G. Velarde, “Internal solitary waves,” *Stud. Appl. Math.* **86**, 167–184 (1992).
- <sup>17</sup>W. B. Zimmerman and M. G. Velarde, “Nonlinear waves in stably stratified dissipative media—Solitary waves and turbulent bursts,” *Phys. Scr.* **T55**, 111–114 (1994).
- <sup>18</sup>V. Nekorkin and M. G. Velarde, “Solitary waves, soliton bound states and chaos in a dissipative Korteweg–de Vries equation,” *Int. J. Bifurc. Chaos* **4**, 1135–1146 (1994).
- <sup>19</sup>M. G. Velarde, V. Nekorkin, and A. G. Maksimov, “Further results on the evolution of solitary waves and their bound states of a dissipative Korteweg–de Vries equation,” *Int. J. Bifurc. Chaos* **5**, 831–839 (1995).
- <sup>20</sup>X. Sun, W. Huang, and J. Cai, “Coexistence of the solitary and periodic waves in convecting shallow water fluid,” *Nonlinear Anal.: Real World Appl.* **53**, 103067 (2020).
- <sup>21</sup>Z. Du, J. Li, and X. Li, “The existence of solitary wave solutions of delayed Camassa–Holm equation via a geometric approach,” *J. Funct. Anal.* **275**(4), 988–1007 (2018).
- <sup>22</sup>Q. Qi, S. Yan, and X. Zhang, “Periodic and solitary waves in a Korteweg–de Vries equation with delay,” *Proc. R. Soc. Edinb. A* **155**, 176–198 (2025).
- <sup>23</sup>F. Fan and M. Wei, “Traveling waves in a quintic BBM equation under both distributed delay and weak backward diffusion,” *Physica D* **458**, 133995 (2024).
- <sup>24</sup>M. Wei, F. Fan, and X. Chen, “Periodic wave solutions for a KP-MEW equation under delay perturbation,” *Physica D* **462**, 134143 (2024).
- <sup>25</sup>A. Chen, L. Guo, and X. Deng, “Existence of solitary waves and periodic waves for a perturbed generalized BBM equation,” *J. Differ. Equ.* **261**, 5324–5349 (2016).
- <sup>26</sup>S. Chen and J. Huang, “Periodic traveling waves with large speed,” *Z. Angew. Math. Phys.* **74**, 102 (2023).

- <sup>27</sup>L. Guo and Y. Zhao, "Existence of periodic waves for a perturbed quintic BBM equation," *Discrete Contin. Dyn. Syst. Ser. A* **40**, 4689–4703 (2020).
- <sup>28</sup>Z. Du and J. Li, "Geometric singular perturbation analysis to Camassa-Holm Kuramoto-Sivashinsky equation," *J. Differ. Equ.* **306**, 418–438 (2022).
- <sup>29</sup>F. Cheng and J. Li, "Geometric singular perturbation analysis of Degasperis-Procesi equation with distributed delay," *Discrete Contin. Dyn. Syst. A* **41**, 967–985 (2021).
- <sup>30</sup>F. Dumortier, R. Roussarie, and J. Sotomayor, "Generic 3-parameter families of vector fields on the plane, unfolding a singularity with nilpotent linear part. The cusp case of codimension 3," *Ergod. Theory Dyn. Syst.* **7**, 375–413 (1987).
- <sup>31</sup>M. Han, *Bifurcation Theory of Limit Cycles* (Science Press, 2013).
- <sup>32</sup>C. Christopher, C. Li, and J. Torregrosa, *Limit Cycles of Differential Equations* (Springer International Publishing, 2024).
- <sup>33</sup>M. Grau *et al.*, "A Chebyshev criterion for Abelian integrals," *Trans. Am. Math. Soc.* **363**, 109–129 (2011).
- <sup>34</sup>N. Fenichel, "Geometric singular perturbation theory ordinary differential equations," *J. Differ. Equ.* **31**, 53–98 (1979).
- <sup>35</sup>M. Han, J. Yang, A. T. Alexandrina, and Y. Gao, "Limit cycles near homoclinic and heteroclinic loops," *J. Dyn. Differ. Equ.* **20**, 923–944 (2008).
- <sup>36</sup>X. Sun and W. Huang, "Bounding the number of limit cycles for a polynomial Lienard system by using regular chains," *J. Symb. Comput.* **79**, 197–210 (2017).